

# Mesospheric Water Vapor in 2022

Gerald E. Nedoluha<sup>1</sup>, R. Michael Gomez<sup>1</sup>, Ian Boyd<sup>2</sup>, Helen Neal<sup>2</sup>, Douglas Ray Allen<sup>3</sup>, Alyn Lambert<sup>4</sup>, and Nathaniel J Livesey<sup>5</sup>

<sup>1</sup>Naval Research Laboratory

<sup>2</sup>Bryan Scientific Consulting

<sup>3</sup>Naval Research Lab

<sup>4</sup>Jet Propulsion Lab (NASA)

<sup>5</sup>Jet Propulsion Laboratory

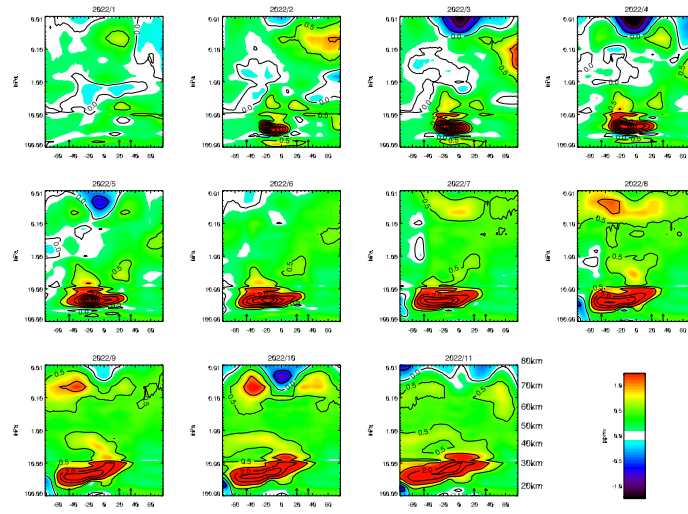
May 5, 2023

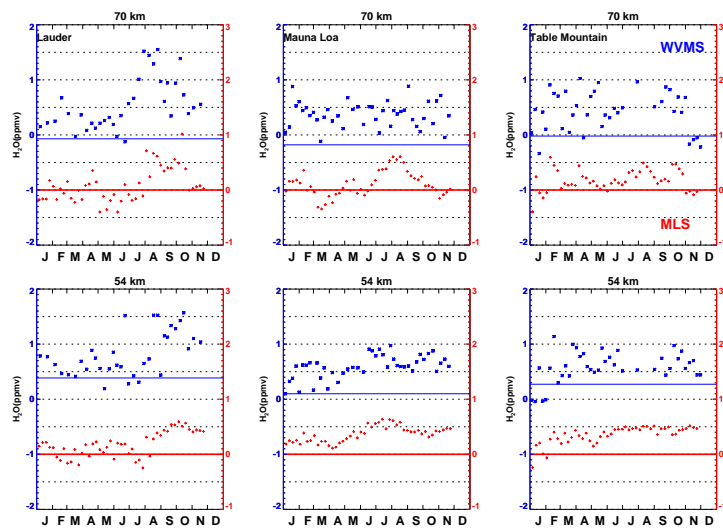
## Abstract

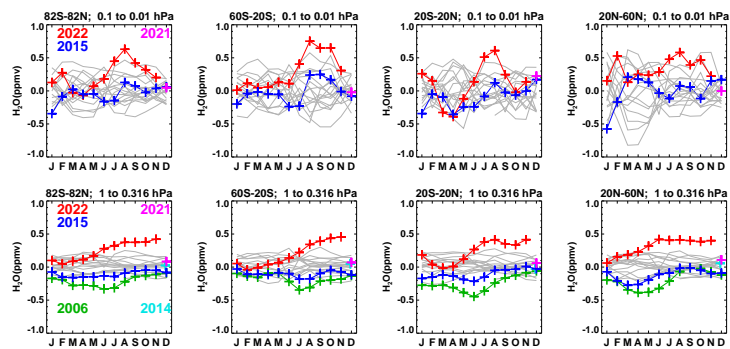
The eruption of the Hunga Tonga undersea volcano in January 2022 injected water vapor to altitudes as high as 53 km, but also an unprecedented and much larger amount of water vapor into the stratosphere. Several months after the eruption, measurements from the Aura Microwave Limb Sounder (MLS) and from three ground-based Water Vapor Millimeter Wave (WVMS) instruments began to measure record-high amounts of water vapor in the mesosphere over a wide range of latitudes. While there are indications that some of this mesospheric increase in water vapor was probably caused by the Hunga Tonga eruption, the dynamical situation in 2022 also played an important part in establishing the unusually large water vapor mixing ratios, both in the upper and lower mesosphere.

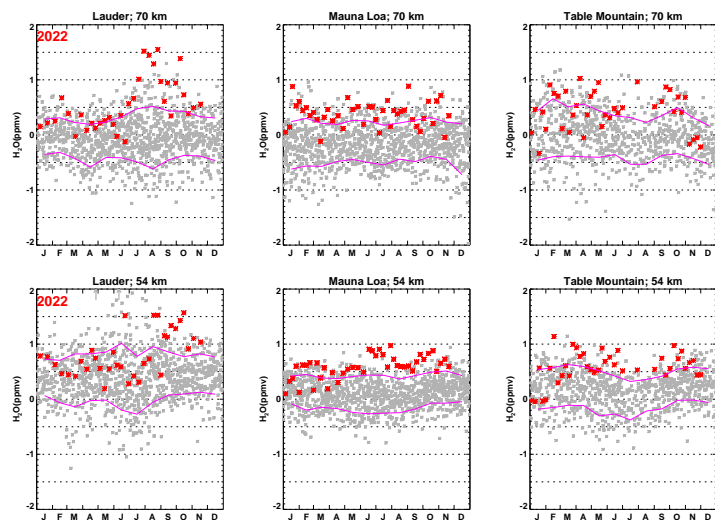
## Hosted file

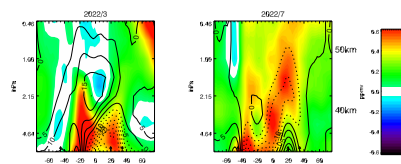
962462\_0\_art\_file\_10949418\_rn1939.docx available at <https://authorea.com/users/563972/articles/641509-mesospheric-water-vapor-in-2022>

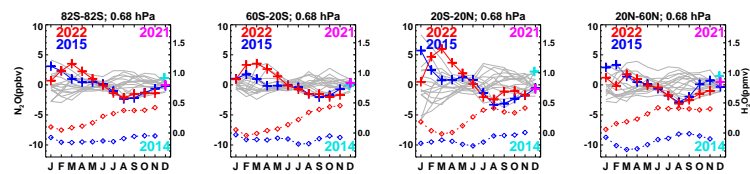


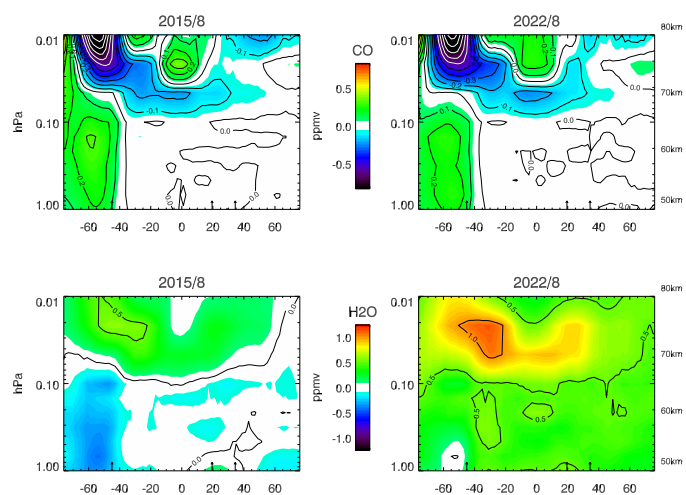




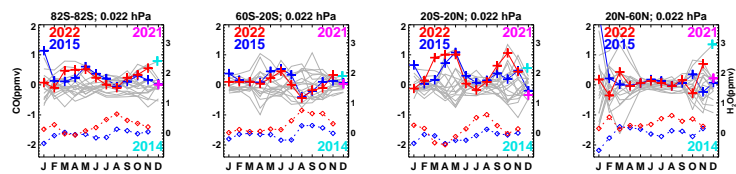












# Mesospheric Water Vapor in 2022

<sup>1</sup>Gerald E. Nedoluha, <sup>1</sup>R. Michael Gomez, <sup>2</sup>Ian Boyd, <sup>2</sup>Helen Neal, <sup>1</sup>Douglas R. Allen, <sup>3</sup>Alyn Lambert, and <sup>3</sup>Nathaniel J. Livesey

<sup>1</sup>Naval Research Laboratory, Washington, DC, USA

<sup>2</sup>Bryan Scientific Consulting LLC, Charlottesville, VA, USA

<sup>3</sup>Jet Propulsion Laboratory, California Institute of Technology, Pasadena, CA, USA

Corresponding author: Gerald Nedoluha (nedoluha@nrl.navy.mil)

## Key Points:

A Aura MLS and three ground-based WVMS instruments all observed record-high water vapor in the upper and lower mesosphere in 2022.

B Some of this mesospheric increase in water vapor was probably caused by the Hunga Tonga eruption.

C Dynamics also played an important part establishing record-high water vapor mixing ratios, both in the upper and lower mesosphere.

## Abstract

The eruption of the Hunga Tonga undersea volcano in January 2022 injected water vapor to altitudes as high as 53 km, but also an unprecedented and much larger amount of water vapor into the stratosphere. Several months after the eruption, measurements from the Aura Microwave Limb Sounder (MLS) and from three ground-based Water Vapor Millimeter Wave (WVMS) instruments began to measure record-high amounts of water vapor in the mesosphere over a wide range of latitudes. While there are indications that some of this mesospheric increase in water vapor was probably caused by the Hunga Tonga eruption, the dynamical situation in 2022 also played an important part in establishing the unusually large water vapor mixing ratios, both in the upper and lower mesosphere.

## Plain Language Summary

The eruption of the Hunga Tonga undersea volcano in January 2022 injected water vapor to altitudes as high as 53 km. While the direct injection to 53 km was impressive, the quantity was insufficient to significantly affect the global mesospheric (~50 km to 80 km) water vapor budget. However, the Hunga Tonga eruption can also affect mesospheric water vapor through the gradual ascent of the unprecedented and much larger amount of water vapor that was directly injected into the stratosphere (~15 km to 50 km). Several months after the eruption, measurements from the Aura Microwave Limb Sounder (MLS) and from three ground-based Water Vapor Millimeter Wave (WVMS) instruments began to measure record-high amounts of water vapor in the mesosphere. While some of this increase is probably caused by the rise of unusually wet air from the Hunga Tonga plume, determining the precise contribution of the plume is difficult because there are a number of other factors that also caused an increase in mesospheric water vapor in 2022.

## 1. Introduction

The January 2022 eruption of the Hunga Tonga undersea volcano, located at 20.5° S, 184.6° E, injected water vapor into the atmosphere that the Aura Microwave Limb Sounder (MLS) measured at altitudes as high as 53 km (~0.5 hPa) [Millán et al, 2022]. Aerosol plume heights at similar altitudes were also reported from GOES-17 and Himawari-8 measurements [Carr et al., 2022]. Initial intrusions of H<sub>2</sub>O into the stratosphere as observed by radiosondes were shown in Vömel et al. [2022].

While the direct injection of water vapor into the lower mesosphere at ~53 km was an impressive event, the injection of a much larger amount of water vapor into the stratosphere is likely to have a much more long-lasting effect on water vapor in the middle atmosphere. Millán et al. [2022] showed the evolution of the stratospheric H<sub>2</sub>O plume from Hunga Tonga through March 2022. Schoeberl et al. [2022] tracked the water vapor and aerosol plumes in the lower stratosphere using MLS and the Ozone Mapping and Profile Suite–Limb Profiler (OMPS-LP) measurements, and both Schoeberl et al [2022] and Khaykin et al. [2022] further modeled the dispersion of the H<sub>2</sub>O plume using model winds. Nedoluha et al. [2023] documented the rise of water vapor anomalies in the stratosphere over Mauna Loa using MLS and ground-based microwave measurements through July 2022, and placed the water vapor variations in that region within the context of previous variations observed since 1996.

In this study we will focus on how the injection of water into the stratosphere may have affected mesospheric water vapor in 2022 in the months following the eruption. We will place the 2022 water vapor measurements into historical context by making use of the multi-decadal databases available from MLS and from each of three ground-based microwave instruments. We will show that, in the second half of 2022, all four of these instruments often recorded the highest water vapor mixing ratio anomalies (relative to local seasonal climatologies) that they had ever observed in the lower mesosphere in the tropics and at Northern and Southern mid-latitudes. In the upper mesosphere record-high mixing ratios were observed in the tropics and at both Northern and Southern mid-latitudes from July to September. While the timing of these record-high mixing ratios in the mesosphere certainly suggest a contribution from the water vapor plume associated with the eruption of Hunga Tonga, we find that the dynamics in 2022 also likely played a role in establishing some of these high mixing ratios.

## **2. Ground-based and Satellite Datasets**

The Water Vapor Mm-wave Spectrometer (WVMS) instruments have been making nearly continuous measurements of water vapor in the middle atmosphere since the early 1990's. Measurements are made from the Network for the Detection of Atmospheric Composition Change (NDACC) sites at Table Mountain, California (34.4° N, 120.5° W), Mauna Loa, Hawaii (19.5° N, 155.6° W), and Lauder, New Zealand (45.0° S, 169.7° E). These instruments make spectrally resolved measurements of the 22 GHz water vapor emission line to obtain a vertical profile of water vapor. Details of the instrumentation and the measurement technique are described in Gomez et al. [2012].

The standard WVMS measurement product, which will be used in this study, is retrieved from a ~1 week integration of the spectrum within +/-30 MHz of the H<sub>2</sub>O emission peak at 22 GHz.

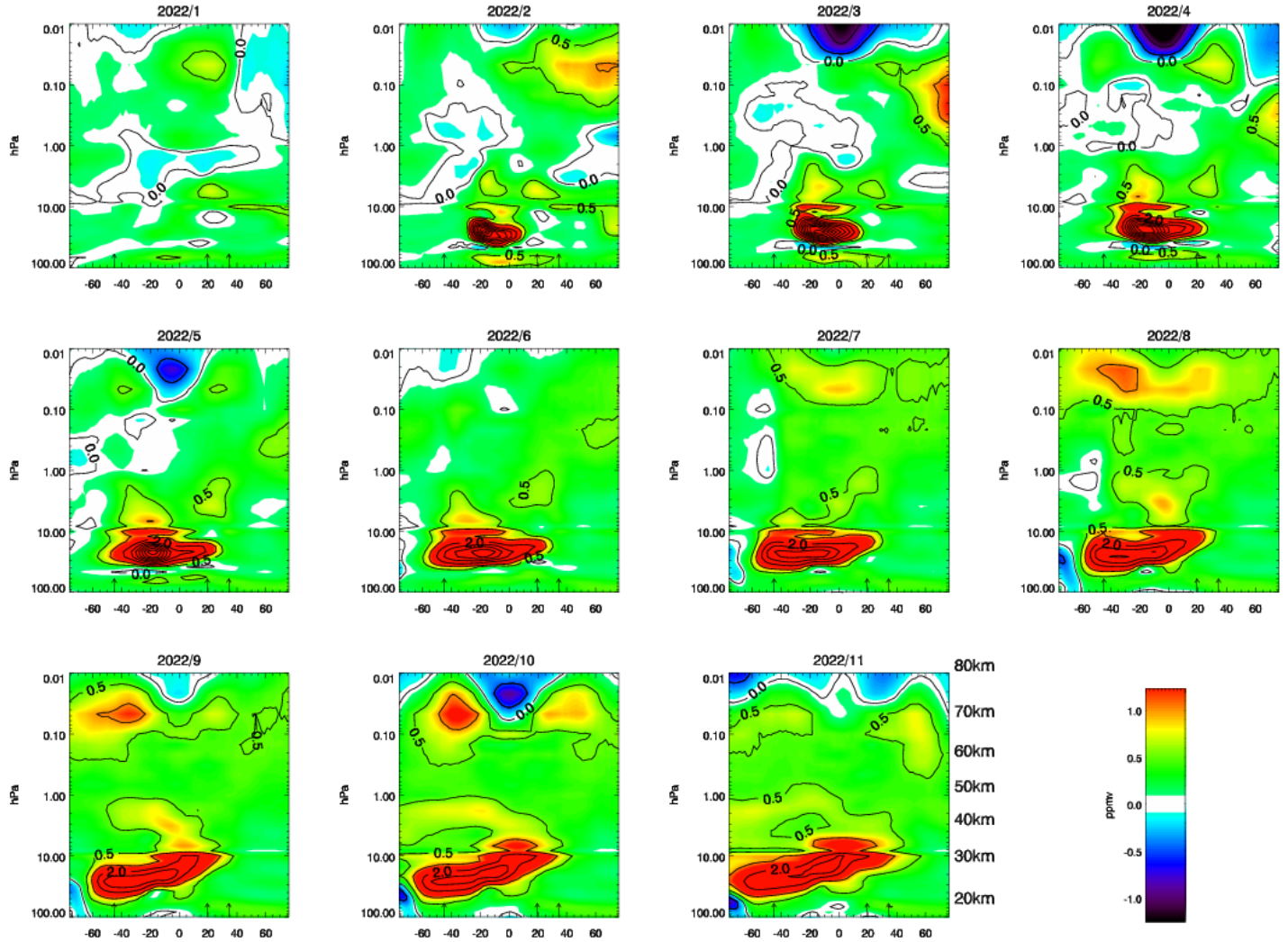
Results from these retrievals from 1992 to 2021 were presented in Nedoluha et al. [2022], where H<sub>2</sub>O vertical profiles were shown from 45 km to 80 km. Here we extend these results through the end of November 2022, except at Mauna Loa, where measurements stop on November 22, 2022, a few days before the lava flow from the Mauna Loa eruption cut power and communication to the site.

The Aura MLS water vapor product is retrieved from the radiances measured by the radiometers centered near 190 GHz. The v2.2 retrievals were validated by Lambert et al. [2007]. The MLS v4 H<sub>2</sub>O retrievals were used in Millán et al. [2022] because of poor fits in v5 retrievals in regions of extremely enhanced H<sub>2</sub>O. In this study we will focus on the plume of enhanced H<sub>2</sub>O months after the eruption, at which point the level of enhancement is not so large as to cause a problem for the v5 retrievals. The v5 retrievals are generally recommended by the MLS Team. Livesey et al. [2021] showed that the v5 retrievals remove an upward drift in the MLS v4 H<sub>2</sub>O measurements of ~2-4%/decade from ~50 hPa to 0.1 hPa since 2010 relative to the Atmospheric Chemistry Experiment Fourier Transform Spectrometer (ACE-FTS) [Bernath, et al., 2005].

The Aura MLS N<sub>2</sub>O and CO products will be used to diagnose dynamical anomalies that affect H<sub>2</sub>O photochemistry. The v5 N<sub>2</sub>O product makes use of the 190 GHz radiances and, like the H<sub>2</sub>O v4 retrievals, suffered some drift. This has been partially corrected in the v5 dataset [Livesey et al., 2021]. The CO measurements are retrieved from radiance measurements of two bands of the 240 GHz radiometer. Details are given in Pumphrey et al. [2007].

### **3. WVMS and MLS Measurements of H<sub>2</sub>O in 2022**

In Figure 1 we show monthly zonal median MLS H<sub>2</sub>O measurement anomalies in the stratosphere and mesosphere for January to November, 2022. We plot a zonal median in order to ensure that a few spurious MLS profiles do not affect the monthly results. The effect of the Hunga Tonga eruption is apparent in the lower stratosphere (below ~10 hPa) during all months except, because we plot zonal medians, in January (the month of the eruption). Throughout this study we will use zonal medians instead of means to ensure that a few spurious measurements do not affect the interpretation. There are increasingly positive anomalies in the upper stratosphere, appearing first in the tropics, and then clearly spreading to higher latitudes in the Southern Hemisphere beginning in August.



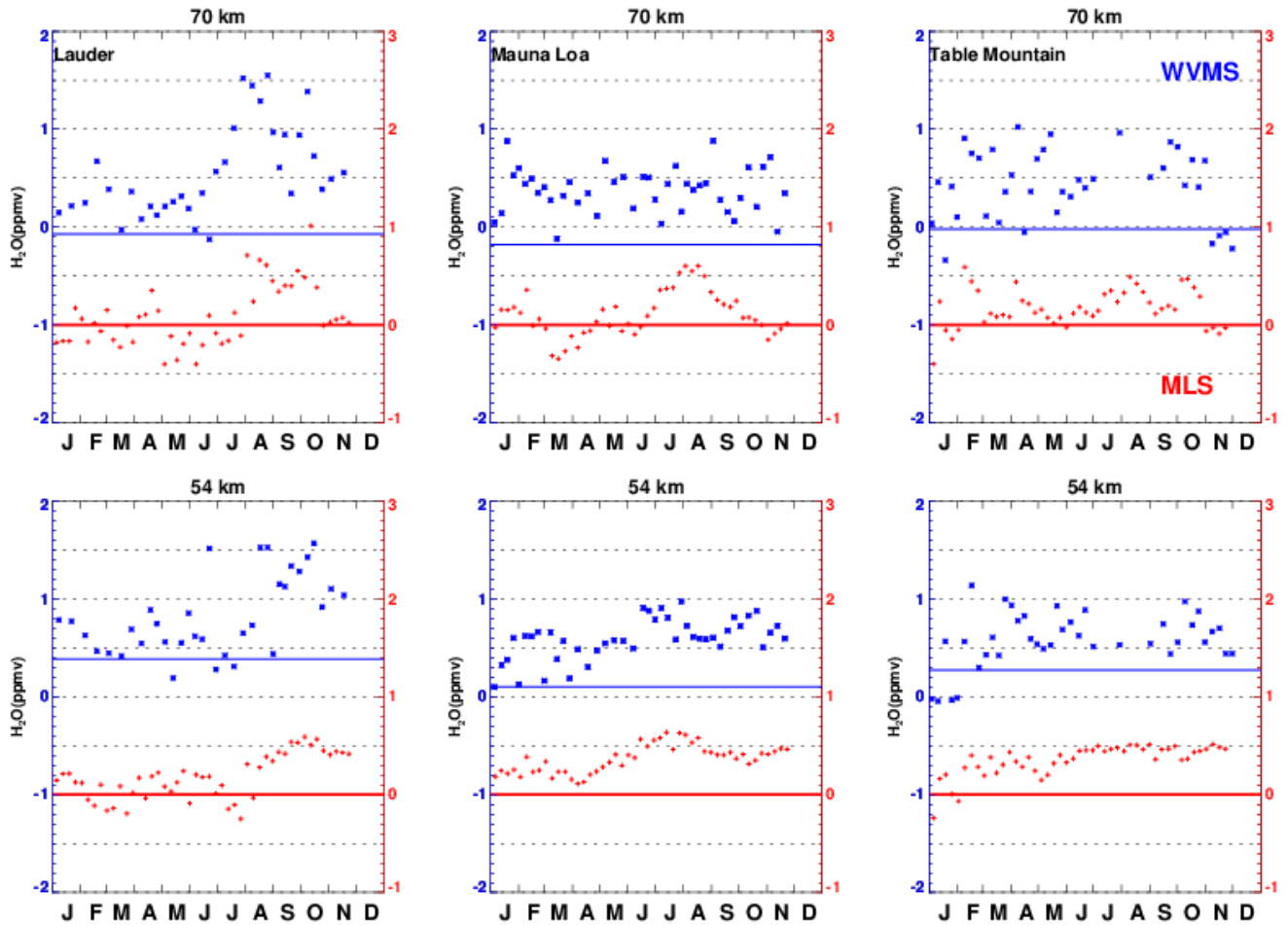
1

**Figure 1**– The monthly zonal-median MLS H<sub>2</sub>O anomaly relative to the monthly MLS climatology for measurements from January to November 2022. Data is shown on the native MLS pressure levels. Indicated altitudes are approximate. The arrows indicate the latitudes of the WVMS sites. Contours are in 0.5 ppmv intervals up to 1 ppmv, and in 1 ppmv intervals for larger mixing ratio anomalies.

In addition to this spread of increased H<sub>2</sub>O in the upper stratosphere, there is an apparent overall increase in water vapor anomaly throughout much of the lower mesosphere (~1 hPa to 0.1 hPa) between January and November 2022. In the upper mesosphere (~0.1 hPa to 0.01 hPa) there is a high water vapor anomaly at Southern mid-latitudes from August to September 2022 which appears at approximately the same time as the upper stratospheric increase. At Northern mid-latitudes water vapor in the upper mesosphere begins the year at below-average levels, increases to above average levels, and then decreases again. Possible causes of all of these variations will be discussed in Section 5.

In Figure 2 we show the water vapor mixing ratio anomalies for 54 km and 70 km (~0.4 and 0.02 hPa) at the three sites as measured by the WVMS instruments, as well as MLS measurements

127 coincident (within  $\pm 2^\circ$  latitude,  $\pm 30^\circ$  longitude) with each site. The WVMS averaging kernel  
 128 at the two altitudes shown has a FWHM of  $\sim 16$  km, hence the 54 km level does include some  
 129 contribution from the upper stratosphere. A typical WVMS averaging kernel for these retrievals  
 130 is shown in Figure 1 of Nedoluha et al. [2022]. The MLS measurements shown in Figure 2 are  
 131 convolved with WVMS averaging kernels, and make use of the same MLS-climatology-based a  
 132 priori ( $x_{MLS}^{climo}$ ) that is used in the WVMS retrievals, i.e.  $x_{sat}^{conv} = x_{MLS}^{climo} + A_{site} \times (x_{sat}^{meas} -$   
 133  $x_{MLS}^{climo})$ . The MLS climatology is calculated using MLS measurements through the end of 2021.  
 134 Throughout this study when we refer to WVMS anomalies this refers to an anomaly calculated  
 135 relative to the MLS climatology which is used as the a priori for the WVMS retrievals, hence the  
 136 average WVMS anomaly may be offset from zero. This difference is indicated in Figure 2 for  
 137 each altitude and site. For Lauder at 54 km this average WVMS anomaly relative to the MLS  
 138 climatology is  $+0.4$  ppmv, and at Table Mountain the offset is  $+0.3$  ppmv. For the other four  
 139 panels it is within the range  $\pm 0.2$  ppmv of zero.



141 **Figure 2-** Water vapor mixing ratio anomalies during 2022 relative to an MLS-based  
 142 climatology at the three WVMS sites. WVMS results (in blue) are  $\sim$ weekly averages. MLS  
 143 results (in red) are weekly averages convolved with WVMS averaging kernels. The blue line  
 144 represents the historical average WVMS anomaly relative to the MLS climatology. To prevent

overplotting the MLS data have been shifted by -1 ppmv relative to WVMS (matching the red scale on the left).

As noted above in the discussion of Figure 1, MLS measured an increase in H<sub>2</sub>O anomalies throughout the lower mesosphere from January to November 2022. The MLS and WVMS results in Figure 2 show an increase in H<sub>2</sub>O mixing ratio anomalies in 2022 at 54 km at all three sites, but the timing of the increase varies with site. At Lauder the WVMS data shows one anomaly of ~1.5 ppmv at 54 km in June, but only after mid-August are the anomalies relative to the MLS climatology consistently larger than 1 ppmv. Similarly, the coincident MLS data shows an increase from July to August. There is also an increase in water vapor in at 70 km that occurs slightly earlier. The MLS anomaly at 70 km is smaller, but, just as for the WVMS measurements, the MLS anomalies at Lauder at 70 km are largest in August and then decrease.

At Mauna Loa, the H<sub>2</sub>O anomalies measured by WVMS at 54 km are all >0.5 ppmv from June onwards. The coincident MLS measurements show a similarly timed increase between April and June. There is a temporary increase in H<sub>2</sub>O at 70 km in the second half of the year in the MLS data coincident with Mauna Loa that is not apparent in the noisier WVMS data, but by November the MLS retrieved mixing ratios are back near the climatological values.

At Table Mountain the mixing ratio anomalies at 54 km as measured by both WVMS and MLS increase from January through March, and then remain elevated throughout the year. The WVMS H<sub>2</sub>O anomalies at 54 km are almost always between ~0.4 to 1.0 ppmv from March onwards with no clear temporal trend. In the less variable convolved MLS anomalies there is a clear small (~0.2 ppmv) increase between the first and second half of the year at 54 km, possibly related to the arrival of increased mixing ratios caused by the eruption. At 70 km over Table Mountain the anomalies measured by both MLS and WVMS are negative or near zero at the beginning of the timeseries in January, and at the end of the timeseries in November. From February through October the 70 km MLS and WVMS retrievals show a positive anomaly.

#### **4. Comparison of Mesospheric H<sub>2</sub>O in 2022 with Previous Years**

In order to better understand the uniqueness of the H<sub>2</sub>O perturbation caused by the injection of the Hunga Tonga eruption we compare the H<sub>2</sub>O anomalies observed in 2022 with H<sub>2</sub>O from previous years in which measurements from MLS are available. We perform this comparison over the full 82° S to 82° N latitude range of the MLS measurements, and over three 40-degree wide zonal regions. These MLS results are reported using two sets of mesospheric pressure ranges, one set in the upper mesosphere, and another set in the lower mesosphere.

While the ground-based WVMS measurements can provide continuous coverage from a single site throughout the day, they clearly provide a much more limited spatial sampling of the atmosphere than the MLS measurements, and the retrievals have a coarser vertical resolution. In addition, there are temporal differences between the datasets, with the WVMS measurements providing data from years before MLS measurements began and into the foreseeable future, but with temporal gaps in ground-based measurements due to adverse weather, instrumental failure, or in some cases absence of an instrument at a particular site. We compare below the unusual

large-scale changes observed by all four instruments with their respective historical datasets, and to compare these with mesospheric H<sub>2</sub>O during 2022.

#### 4.1 Comparison of MLS Measurements from 2022 with Previous Years

In Figure 3 we show monthly-mean MLS H<sub>2</sub>O anomalies since 2004 calculated from area weighted zonal medians over latitudinal ranges. We show a lower mesospheric mixing ratio anomaly, which is the average of the four reported MLS levels from 1 hPa to 0.316 hPa (~48 km to ~58 km). We find that the magnitude of the H<sub>2</sub>O anomaly is not very sensitive to the precise choice of levels in the lower mesosphere. For the upper mesosphere we use the four levels from 0.1 hPa to 0.01 hPa (~64 km to ~78 km). Both of these pressure ranges are chosen to be approximately centered around the altitudes used in Figure 2.

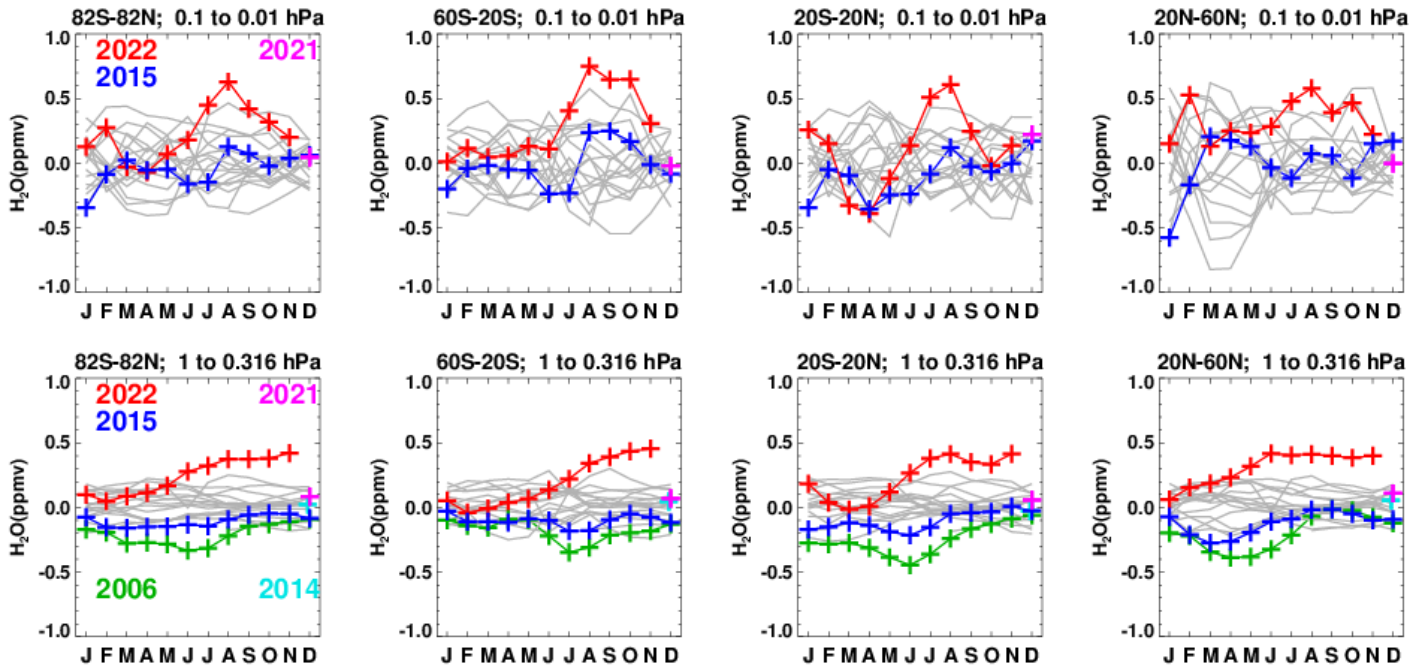


**Figure 3** – MLS monthly median water vapor anomalies in the upper mesosphere (top; 0.1 to 0.01 hPa) and lower mesosphere (bottom; 1 to 0.316 hPa) relative to an MLS climatology. Results are area-weighted and are shown for all MLS measurement latitudes, and for three latitude bands. Monthly measurements for each year are shown in gray, except for measurements from 2022 which are shown in red, measurements from 2015 which are shown in blue, and measurements from December 2021, before the eruption, which are shown in pink. In the lower mesosphere we also highlight measurements from 2006 in green, and measurements from December 2014 in cyan. Note that since these are derived from monthly zonal medians, the tick marks are placed at the center of each month (unlike Figure 2).

The 82° S to 82° N MLS lower mesospheric H<sub>2</sub>O anomaly in 2022 starts slightly above average, and then grows until it exceeds the 2004-2021 historically measured range of mixing ratios from



June 2022 onwards. From July 2022 onwards, the lower mesospheric mixing ratio anomaly exceeds the historical range in all three regions. The 20° N to 60° N lower mesospheric H<sub>2</sub>O mixing ratios for 2022 exceed the historical range earlier than at the other latitudes. Schoeberl et al. [2022] tracked the dispersal of the plume in the upper stratosphere using forward domain filling with Modern-Era Retrospective analysis for Research and Applications (MERRA)-2 winds, and showed that while there was rapid spread from 20° S to Northern midlatitudes there was very little spread to Southern midlatitudes. Khaykin et al. [2022] calculated the water vapor dispersion from the MLS plume using the Chemical Lagrangian Model of the Stratosphere (CLaMS) and showed a similar dispersion pattern. This asymmetry in the dispersion may explain in part the interhemispheric difference in the timing of the lower mesospheric increase. An unexplained feature, however, is the decrease in the H<sub>2</sub>O anomaly in 2022 from 20° S to 20° N that occurs from January to March in the lower mesosphere, and from January to April in the upper mesosphere. Results from 2015 will be highlighted for comparison with 2022 throughout much of this manuscript since the QBO-phase variation during 2015, and hence at least some of the stratospheric and mesospheric dynamics, was quite similar to that of 2022 [Nedoluha et al., 2023]. We will discuss the influence of effects on all of these anomalies in Section 5.

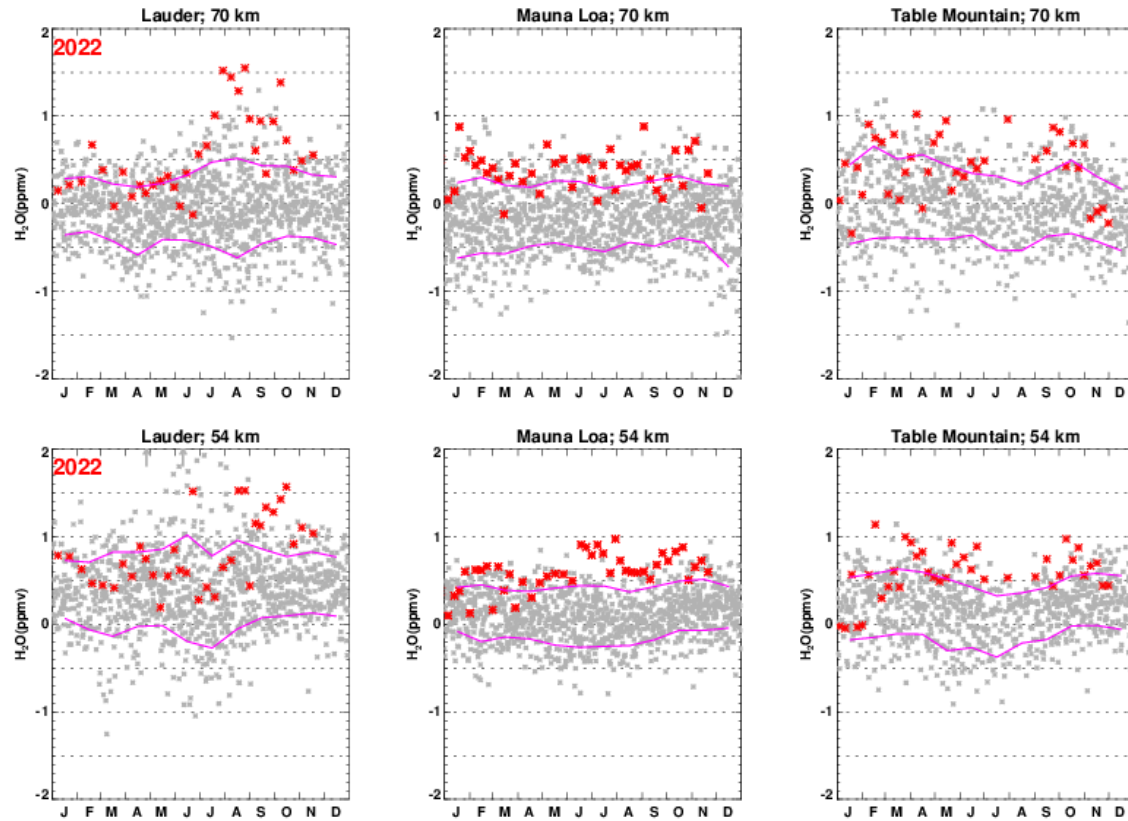
Water vapor mixing ratio anomalies for 2006 in the lower mesosphere are highlighted to put the eruption induced perturbations from 2022 into perspective relative to other geophysical variations that affect mesosphere H<sub>2</sub>O. Anomalies for 2006 are highlighted to emphasize that H<sub>2</sub>O mixing ratios over large regions, and even globally, can for several months have mixing ratios that are consistently the lowest among the 18 years of MLS measurements, even in the absence of a major event such as the Hunga Tonga eruption that affects H<sub>2</sub>O. The low H<sub>2</sub>O values in 2006 were previously noted in Nedoluha et al. [2013] as having followed several years of low tropical tropopause temperatures. Fueglistaler et al. [2013] documented the effect of tropical tropopause temperatures on stratospheric H<sub>2</sub>O during this period, and showed the ascent of the unusually dry air during the years before 2006.

Figure 3 shows that the anomaly variations in the upper mesosphere are larger and more variable from month-to-month than in the lower mesosphere. As is the case in the lower mesosphere, the near-global upper mesospheric mixing ratios in 2022 exceed the 2004-2021 levels beginning in July. However, except at the Southern midlatitudes, the levels fall back within the 2004-2021 range by October 2022. In addition to highlighting 2022, the anomalies for 2015 in the upper mesosphere have been highlighted in Figure 3. While the mixing ratios in the upper mesosphere in 2015 are lower than in 2022, they also show a similar positive increase in August in the Southern midlatitudes. Possible geophysical causes of these upper mesospheric variations are discussed in Section 5.

## 4.2 Comparison of WVMS Measurements from 2022 with Previous Years

In Figure 4 we show all ~weekly WVMS H<sub>2</sub>O retrieval anomalies as a function of time-of-year. The retrievals are obtained from several decades of measurements from all three sites. The WVMS data set from Lauder begins in November 1992, while that from Mauna Loa starts in November 1996. The WVMS data set from Table Mountain begins in May 1993, but there are no measurements from 1998-2003 and 2006-2009. Details of data availability are given in

Nedoluha et al. [2022]. Unlike MLS measurements, which are available nearly every day, WVMS retrievals are somewhat weather dependent, and this causes some variation in the time required to obtain a retrieval. Unlike Figure 3, we have therefore not binned the results by month since the ~weekly integration periods required to obtain retrievals could result in a monthly data point including anywhere from one to five retrievals for each year.



**Figure 4-** WVMS ~weekly water vapor retrieval anomalies relative to an MLS-based climatology. Measurements are shown in gray, except for measurements from 2022 which are shown in red. Two 1992-2021 points fall outside the range shown and are indicated by arrows. The solid pink lines show  $\pm 1\sigma$  from the mean, based on all available measurements for each month.

At Lauder, there are large variations in June and July at 54 km in many years, hence the single large positive anomaly observed in June 2022 at 54 km is not a particularly unusual geophysical variation for this time-of-year. However, from the beginning of September 2022 onwards the retrieved  $H_2O$  anomalies at 54 km are all at least  $1\sigma$  above the mean for that time-of-year. At 70 km in 2022 all but one WVMS measurements are at least  $1\sigma$  above the mean from July onwards.

At Mauna Loa the WVMS  $H_2O$  at 54 km is always  $1\sigma$  above the mean from May 2022 onwards. At 70 km the WVMS measured mixing ratios at Mauna Loa are often more than  $1\sigma$  above the mean, but these high mixing ratios are consistent throughout the year without any apparent trend in 2022. The temporal evolution of the Table Mountain measurements is not dissimilar from those at Mauna Loa. From April until early November 2022, the mixing ratios measured by

WVMS at 54 km at Table Mountain are above, or very near to,  $1\sigma$  above the mean. At 70 km slightly more than half of the measurements show  $\text{H}_2\text{O}$  mixing ratios larger than  $1\sigma$  above the mean throughout 2022. However, in November 2022 there is a sudden drop in the 70 km mixing ratio anomaly to values near the mean. The drop in  $\text{H}_2\text{O}$  mixing ratios from January to March 2022 in the  $20^\circ \text{ S}$  to  $20^\circ \text{ N}$  latitude range shown in Figure 3 is not apparent in either the WVMS Mauna Loa measurements or in the coincident MLS measurements at 54 km. There is a clear minimum in the March 2022 MLS measurements at 70 km, and the lower WVMS measurement in 2022 at 70 km also occurs in March. According to the MLS measurements shown in Figure 1 this drop is most pronounced at latitudes nearest to the equator, so measurements at Mauna Loa are only capturing the northern edge of this tropical variation.

At Lauder, which at  $45^\circ \text{ S}$  is roughly near the middle of the  $20^\circ \text{ S}$  to  $60^\circ \text{ S}$  latitude bin used in Figure 3, the 2022 mixing ratio anomalies at 54 km are from mid-August onwards are, with one exception, at least  $1\sigma$  above the mean. This is similar to the period for which the 2022 lower mesospheric bin of monthly MLS measurements are above the historical envelope of measurements. The WVMS results at 70 km also show variations that are similar to the MLS upper mesospheric measurements shown in Figure 3. The 2022 WVMS 54 km measurements at Mauna Loa and Table Mountain are almost always more than  $1\sigma$  above the mean from May onwards, while the comparable MLS measurements are above the historical envelope from either July onwards or April onwards for the  $20^\circ \text{ S}$  to  $20^\circ \text{ N}$  and  $20^\circ \text{ N}$  to  $60^\circ \text{ N}$  latitudinal ranges respectively. The 2022 WVMS 70 km retrievals at Mauna Loa and Table Mountain are, just like the upper mesospheric  $20^\circ \text{ N}$  to  $60^\circ \text{ N}$  MLS retrievals, high throughout that year. At Table Mountain the 70 km retrievals are always more than  $1\sigma$  above the mean from July through September, the same period during which the comparable  $20^\circ \text{ N}$  to  $60^\circ \text{ N}$  MLS retrievals are above the historical envelope.

All three ground-based WVMS instruments confirm the MLS measurements which show that, in the tropics and at midlatitudes, water vapor mixing ratio anomalies reached unprecedented levels in 2022.

## 5. Effects of Transport and the Solar Cycle on Mesospheric $\text{H}_2\text{O}$

In Figure 1 there are positive  $\text{H}_2\text{O}$  anomalies in the tropical upper stratosphere throughout 2022, and since these are directly above the large positive  $\text{H}_2\text{O}$  anomaly in the mid-stratosphere from the Hunga Tonga plume, these might be interpreted as being directly related to ascent of that plume. However, a precise determination of the spread of  $\text{H}_2\text{O}$  from the Hunga Tonga plume is complicated by the formation of  $\text{H}_2\text{O}$  through the oxidation of  $\text{CH}_4$  which takes place in the stratosphere. The amount of  $\text{CH}_4$  oxidation is dependent upon the rate of ascent, with a slower ascent rate providing more time for the production of  $\text{H}_2\text{O}$ . While MLS does not measure  $\text{CH}_4$ , it does measure  $\text{N}_2\text{O}$ , with which it is strongly correlated [cf. Minschwaner and Manney, 2014]. To illustrate this we show, in Figure 5, the monthly  $\text{H}_2\text{O}$  and  $\text{N}_2\text{O}$  anomalies measured by MLS in the upper stratosphere and lower mesosphere in March and July 2022. In March there is a positive  $\text{H}_2\text{O}$  anomaly in the upper stratosphere at  $20^\circ \text{ S}$ , coinciding with the latitude of Hunga Tonga, which is not anti-correlated with  $\text{N}_2\text{O}$ . However, other large positive anomalies in stratospheric  $\text{H}_2\text{O}$ , such as is seen in the mid-stratosphere in the Northern midlatitudes in March,

and in both hemispheres in July, are coincident with negative N<sub>2</sub>O anomalies. This indicates that, at least to some extent, some of these positive anomalies in H<sub>2</sub>O are caused by an anomalous amount of CH<sub>4</sub> oxidation associated with slow ascent.

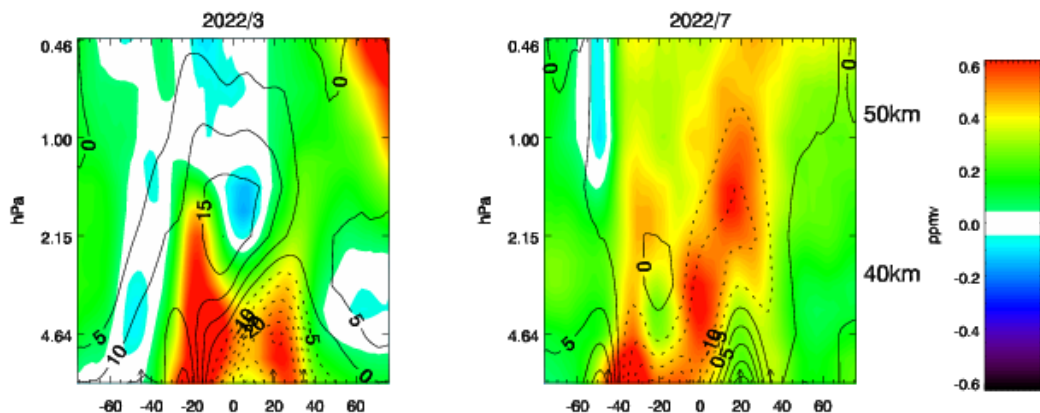


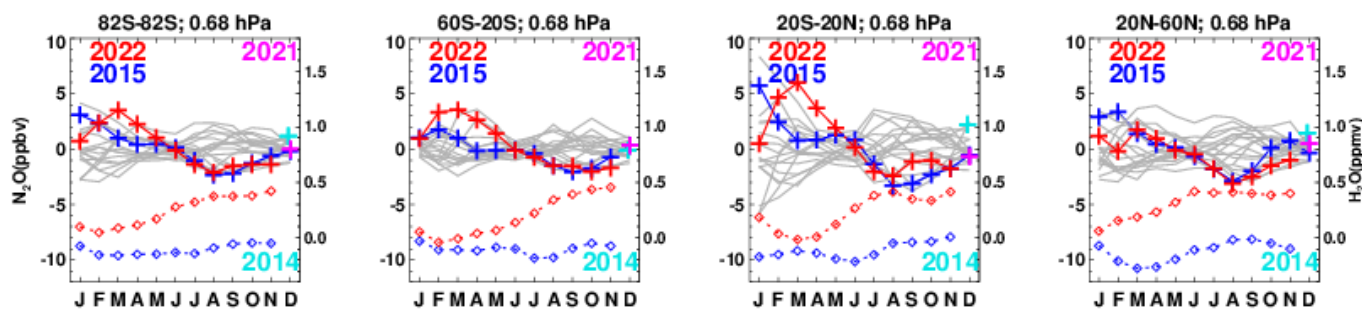
**Figure 5-** Monthly median anomalies of MLS H<sub>2</sub>O (colors) and N<sub>2</sub>O (lines). N<sub>2</sub>O contour lines are in steps of 5 ppbv with negative values dashed. Note that the color scale used here for H<sub>2</sub>O is compressed relative to that used in Figure 1.

In Figure 6 we show MLS N<sub>2</sub>O anomalies at 0.68 hPa for all years, highlighting 2015 and 2022. The N<sub>2</sub>O anomalies in this figure can be compared with the H<sub>2</sub>O anomalies in Figure 3, and we have included the 2015 and 2022 lower mesospheric H<sub>2</sub>O anomalies in Figure 6 to aid this comparison. We have chosen to show the N<sub>2</sub>O anomaly at a single level because of the coarser vertical resolution of the N<sub>2</sub>O retrieval (~8 km FWHM) relative to the H<sub>2</sub>O (~3 km FWHM) at this altitude. The month-to-month variations in H<sub>2</sub>O and N<sub>2</sub>O in 2022 are clearly anticorrelated, and the decrease in anomalous H<sub>2</sub>O observed in the lower mesosphere from January through March is almost certainly caused by a decrease in anomalous CH<sub>4</sub> oxidation in this region. The correlation coefficient between the monthly H<sub>2</sub>O and N<sub>2</sub>O anomalies in the tropics is  $r = -0.97$ , which suggests that almost all of the observed increase in water vapor in the tropics from March to November 2022 is caused by increased CH<sub>4</sub> oxidation resulting from slower ascent. These variations are therefore not likely to be caused by the Hunga Tonga plume. If there were any correlation between H<sub>2</sub>O and N<sub>2</sub>O in the lower mesosphere this might be expected to be positive, since faster ascent might be expected to bring younger, wetter, stratospheric air into the mesosphere. In the Southern and Northern midlatitudes the correlation coefficients are  $r = -0.94$  and  $r = -0.79$  respectively, again suggesting that the dominant cause of the H<sub>2</sub>O variation is CH<sub>4</sub> oxidation. The correlations during other years are not as strong, which is surprising since, as is shown in Figure 5 (albeit in the upper stratosphere and not the mesosphere), it is precisely in the region affected by the Hunga Tonga plume that the anticorrelation between H<sub>2</sub>O and N<sub>2</sub>O is expected to be weakest.

While the variation in the month-to-month H<sub>2</sub>O in 2022 is strongly anticorrelated with N<sub>2</sub>O, there are differences between the H<sub>2</sub>O measurements in 2022 and those in 2015 even when the N<sub>2</sub>O during those two years is very similar. This is most clearly seen in the Northern

341 midlatitudes where the  $\text{N}_2\text{O}$  mixing ratio anomalies in 2015 and 2022 agree to within 0.5 ppbv  
 342 from March through September, while the  $\text{H}_2\text{O}$  remains consistently  $0.48 \pm 0.04$  ppmv larger in  
 343 2022 than in 2015. The origin of this 0.48 ppmv difference in  $\text{H}_2\text{O}$  is of interest. The December  
 344 2021 and December 2014  $\text{N}_2\text{O}$  anomalies are quite similar in both the Northern and Southern  
 345 midlatitudes, as are the January 2022 and January 2015  $\text{N}_2\text{O}$  anomalies. All of these are within  
 346  $\pm 1$  ppbv. During these months the  $\text{H}_2\text{O}$  values (recall that these are all medians, hence the  
 347 plume has little effect on January 2022  $\text{H}_2\text{O}$  values) all differ by  $< 0.09$  ppmv. Thus, before the  
 348 Hunga Tonga eruption, the difference between 2022 and 2015  $\text{H}_2\text{O}$  values in these regions was  
 349 much smaller than that observed in the Northern midlatitudes from March through September.  
 350 This implies that the Hunga Tonga plume may have caused an increase of  $\sim 0.4$  ppmv in  $\text{H}_2\text{O}$  in  
 351 the lower mesosphere between January and March 2022, after which no further plume-induced  
 352 increase occurred in this region. This is consistent with the Schoeberl et al. [2022] calculation  
 353 showing that parcels did spread quite rapidly from the eruption latitude of  $20^\circ \text{S}$  to Northern  
 354 midlatitudes in the upper stratosphere.

355 While the Hunga Tonga eruption probably contributed to this increase in lower mesospheric  $\text{H}_2\text{O}$   
 356 in 2022, we do note that there are two other geophysical drivers that may be playing a role in  
 357 creating the higher mixing ratios in 2022 relative to 2015. As was noted in Nedoluha et al.  
 358 [2023] from 2015 to 2022 the increase in anthropogenic  $\text{CH}_4$  emission could, if the  $\text{CH}_4$  is  
 359 completely oxidized, lead to an increase of up to  $\sim 0.15$  ppmv in  $\text{H}_2\text{O}$  over this 7 year period.  
 360 The strong correlation between  $\text{N}_2\text{O}$  and  $\text{H}_2\text{O}$  in Figure 6 does, however, indicate that at these  
 361 levels not all of the  $\text{CH}_4$  has been oxidized. Also, the tropical tropopause temperatures in the 3  
 362 years leading up to January 2015 were  $\sim 0.7 \text{ K}$  colder than in the 3 years leading up to January  
 363 2022. The resulting difference in dehydration at the tropical tropopause and resulting  $\text{H}_2\text{O}$   
 364 entering the lower stratosphere may contribute to the higher  $\text{H}_2\text{O}$  mixing ratios near the  
 365 stratopause in 2022.

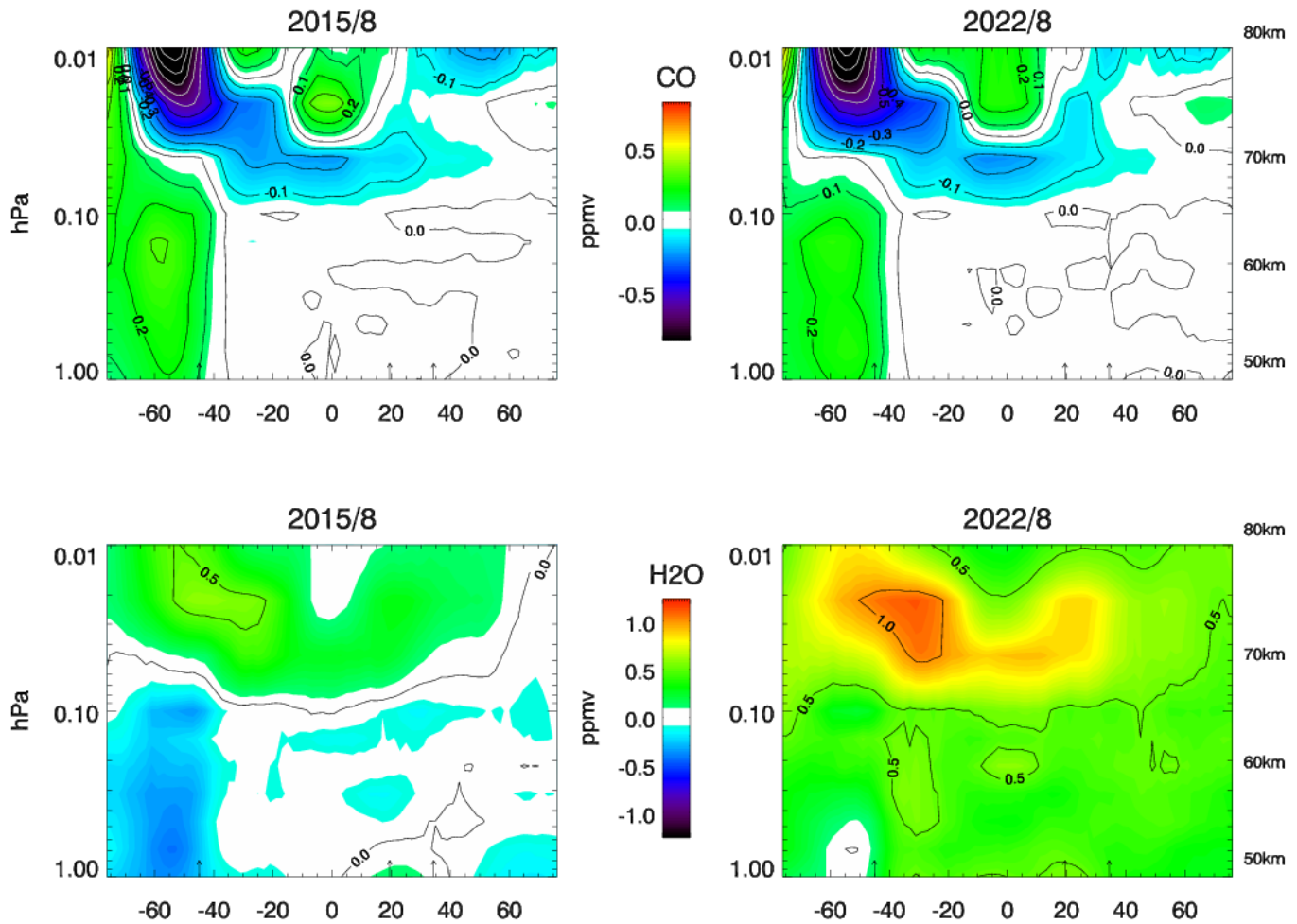


367 **Figure 6-** Monthly median MLS  $\text{N}_2\text{O}$  anomalies at 0.68 hPa. Results are area-weighted and are  
 368 shown for all MLS measured latitudes, and for three latitude bands. Monthly measurements for  
 369 each year are shown in gray, except for measurements from 2022 which are shown in red and  
 370 measurements from 2015 which are shown in blue. December 2021, before the eruption, is  
 371 shown in pink, and December 2014 is shown in cyan. The red and blue diamonds show the  
 372 monthly lower mesospheric  $\text{H}_2\text{O}$  anomalies for 2015 and 2022 from Figure 3 and are referenced  
 373 to the right-hand y-axes.

In the upper mesosphere variations in Lyman-  $\alpha$  irradiance play a role in determining H<sub>2</sub>O mixing ratios [Nedoluha et al., 2009; Remsberg, 2010; Remsberg et al., 2018]. The typical range of Lyman- $\alpha$  irradiance from solar minimum to solar maximum is  $\sim 0.006$  to  $0.009$  W/m<sup>2</sup>, and it is  $0.00740$  W/m<sup>2</sup> in August 2015 and  $0.00778$  W/m<sup>2</sup> in August 2022 (lasp.colorado.edu/lisird/data/composite\_lyman\_alpha) [Machol et al., 2019]. Hence in both years the Lyman- $\alpha$  irradiance is near the mid-range between solar maximum and minimum. Since mesospheric H<sub>2</sub>O is anti-correlated to Lyman- $\alpha$  the effect of the slightly lower Lyman- $\alpha$  irradiance in 2015 would result in H<sub>2</sub>O in August 2015 being just slightly higher than in August 2022. A calculation of the linear fit of the monthly upper mesospheric water vapor as defined in Figure 3 (i.e. the average from 0.1 to 0.01 hPa) to the monthly Lyman- $\alpha$  irradiance for the years 2004 to 2021 shows that the water vapor at solar minimum is  $\sim 0.06$  ppmv higher than at solar maximum, while in the lower mesospheric levels shown in Figure 3 this difference is  $< 0.01$  ppmv. Hence, while the solar cycle does play an important role in establishing H<sub>2</sub>O variations in the upper mesosphere, it is by no means a dominant cause of monthly variations.

In Figure 7 we show MLS measurements of both H<sub>2</sub>O and CO for August of 2015 and 2022. CO is a good dynamical tracer in the upper mesosphere, where the vertical gradient of CO is very steep and of the opposite sign to that of H<sub>2</sub>O in this region. CO is positively correlated with the solar cycle [Lee et al., 2013; Karagodin-Doyennel et al., 2021], but again we note that Lyman- $\alpha$  irradiance in August 2015 and 2022 is similar, so the similarities in the anomalies in CO suggest that the dynamical situation in August of these two years is quite similar in the upper mesosphere. In 2015 the regions of negative CO anomalies from 0.10 to 0.01 hPa correspond approximately with the region of positive H<sub>2</sub>O anomalies, while in 2022 the H<sub>2</sub>O mixing ratios vary similarly, but at a level  $\sim 0.5$  ppmv higher than in 2015. The extremely high H<sub>2</sub>O anomalies observed in the upper mesosphere in August 2022 in the Southern midlatitudes, and at Lauder, are thus, at least to some extent caused by the dynamical conditions during this period, but there are additional geophysical mechanisms that apparently cause a further increase in H<sub>2</sub>O during 2022.





402 **Figure 7**– Monthly zonal-mean MLS CO (top) and H<sub>2</sub>O (bottom) anomalies relative to the MLS  
 403 monthly climatologies for August 2015 (left) and August 2022 (right). Data is shown on the  
 404 native MLS pressure levels. Indicated altitudes are approximate. The arrows indicate the  
 405 latitudes of the WVMS sites.

406 In Figure 8 we show monthly median MLS CO anomalies that can be compared to the upper  
 407 mesospheric H<sub>2</sub>O anomalies shown in Figure 3. We have included in Figure 8 the 2015 and  
 408 2022 upper mesospheric H<sub>2</sub>O anomalies to aid this comparison. The anti-correlation is visibly  
 409 apparent in 2015, where  $r = -0.87$ ,  $-0.65$ , and  $-0.90$  for  $60^\circ \text{ S}$  to  $20^\circ \text{ S}$ ,  $20^\circ \text{ S}$  to  $20^\circ \text{ N}$ , and  $20^\circ \text{ N}$   
 410 to  $60^\circ \text{ N}$  respectively. The high correlation in the northern latitudes is partially due to the very  
 411 high CO and very low H<sub>2</sub>O in January 2015 in this region. In 2022 the correlation coefficients  
 412 for these same latitude bands are  $r = -0.74$ ,  $-0.80$ , and  $-0.67$  respectively. Unlike the case for  
 413 anticorrelation between H<sub>2</sub>O and N<sub>2</sub>O in the lower mesosphere, the anticorrelation between H<sub>2</sub>O  
 414 and CO in the upper mesosphere in 2022 is not unusually strong as compared to those in other  
 415 years.

416 The large increase in H<sub>2</sub>O that is most pronounced at  $20^\circ \text{ S}$  to  $20^\circ \text{ N}$  from April to August 2022  
 417 at 0.1 to 0.01 hPa is correlated with a decrease in CO at those latitudes over the same months,  
 418 and is therefore at least partially caused by anomalous dynamics during those months which

results in the presence of an unusual amount of high H<sub>2</sub>O mixing ratio air from lower altitudes. However, it is also true that, in regions and periods with similar CO anomalies, the upper mesospheric H<sub>2</sub>O mixing ratios in 2022 are larger than in 2015, especially towards the end of the year. From February to April at 60° S to 20° S the CO anomalies for these two years were all similar (within 0.052 ppmv), and the H<sub>2</sub>O in 2022 was, averaged over these three months, only 0.11 ppmv higher. However, in August, when the CO anomalies in all three regions in 2015 and 2022 were again similar (within 0.050 ppmv), the difference in H<sub>2</sub>O anomalies was 0.51 ppmv, 0.49 ppmv, and 0.51 ppmv in the three regions respectively. This suggests that some increase in upper mesospheric H<sub>2</sub>O may have occurred that is not caused by dynamical variations.

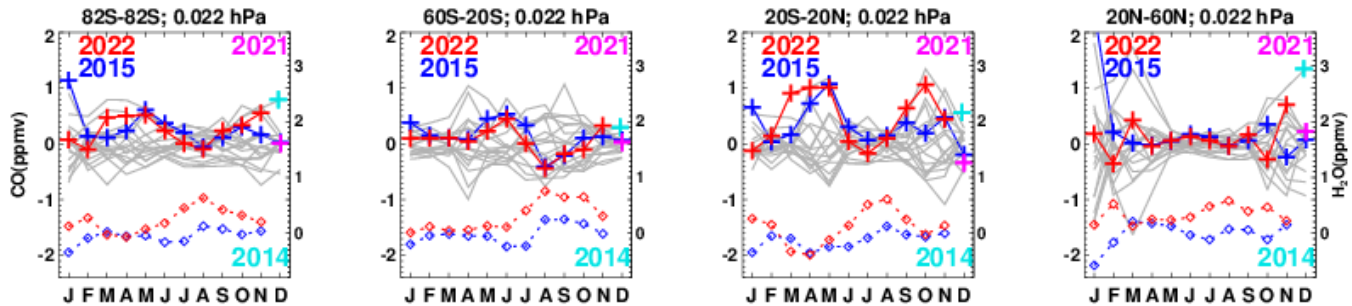


**Figure 8-** Monthly mean MLS CO anomalies at 0.022 hPa. Results are area-weighted and are shown globally for three latitude bands. Monthly measurements are shown in gray, except for measurements from 2022 which are shown in red, measurements from 2015 which are shown in blue, and measurements from December 2021, before the eruption, which are shown in pink. The red and blue diamonds show the monthly lower mesospheric H<sub>2</sub>O anomalies for 2015 and 2022 from Figure 3 and are referenced to the right-hand y-axes.

## 6. Summary

We have shown that H<sub>2</sub>O measurements from MLS and from three WVMS instruments display similar variations of mesospheric H<sub>2</sub>O. Comparisons of the mesospheric H<sub>2</sub>O measured in 2022 with the multi-decadal historical databases from all four of these instruments show, in the second half of 2022, record-high mixing ratios in the tropics, and both Northern and Southern midlatitudes, and in both the lower and upper mesosphere.

The cause of these large H<sub>2</sub>O mixing ratios in the lower mesosphere in the second half of 2022 was shown to be caused, at least in part, by dynamical conditions that allowed for an anomalous amount of CH<sub>4</sub> oxidation and thus increased H<sub>2</sub>O. Particularly surprising is a very strong anti-correlation ( $r = -0.97$ ) between tropical lower mesospheric H<sub>2</sub>O and N<sub>2</sub>O, which is a good tracer of dynamics in this region. This strong anti-correlation suggests that the month-to-month H<sub>2</sub>O variations in this region are almost entirely caused by dynamical variations. However, comparisons between H<sub>2</sub>O in 2015 and 2022, years during which several months showed very similar N<sub>2</sub>O values, show that the H<sub>2</sub>O mixing ratios under similar dynamical conditions were higher in 2022 (by 0.48 $\pm$ 0.04 ppmv in the Northern midlatitudes, whereas the N<sub>2</sub>O values from the two years are very similar from March through September). While this increase from 2015 to 2022 is probably caused in part by the Hunga Tonga eruption, increased anthropogenic CH<sub>4</sub>



emission and differences in tropical tropopause temperatures in the preceding years may also play a significant role.

In the upper mesosphere from February to April, during periods when the dynamical conditions were similar (according to CO tracer measurements) H<sub>2</sub>O was 0.11 ppmv higher in 2022 than in 2015. In August 2015 and 2022 the dynamical conditions were similar and conducive to unusually large water vapor mixing ratios, especially in the Southern midlatitudes. If we compare H<sub>2</sub>O mixing ratios in during these months the record-high H<sub>2</sub>O mixing ratio anomaly in 2022 is ~0.5 ppmv higher in 2022 than in 2015.

## 6. Acknowledgments

We thank G. Rose, M. Kotkamp, M. Brewer, and J. Robinson for their efforts to maintain and calibrate the WVMS instruments at Mauna Loa, Table Mountain, and Lauder. This work was supported by the NASA Earth Sciences Division Upper Atmosphere Research Program and by the Office of Naval Research. Work at the Jet Propulsion Laboratory, California Institute of Technology, was carried out under a contract with the National Aeronautics and Space Administration. We thank M. Heney for making the daily GMA:GEOS5 temperature data at each site available in a convenient form.

## 7. Data Availability Statement

WVMS weekly retrievals are available on the NDACC data server at [www-air.larc.nasa.gov/missions/ndacc/data.html#](http://www-air.larc.nasa.gov/missions/ndacc/data.html#). MLS v5 data are available at [disc.gsfc.nasa.gov/datasets?page=1&keywords=ML2H2O\\_005](http://disc.gsfc.nasa.gov/datasets?page=1&keywords=ML2H2O_005). GEOS temperature data are available at [gmao.gsfc.nasa.gov/GMAO\\_products/](http://gmao.gsfc.nasa.gov/GMAO_products/).

## 8. References

- Bernath, P. F., et al.: Atmospheric Chemistry Experiment (ACE): Mission overview (2005), *Geophys. Res. Lett.*, 32, L15S01, <https://doi.org/10.1029/2005GL022386>, 2005.
- Carr, J. L., Horváth, Á., Wu, D. L., & Friberg, M. D. (2022). Stereo plume height and motion retrievals for the record-setting Hunga Tonga-Hunga Ha'apai eruption of 15 January 2022. *Geophysical Research Letters*, 49, e2022GL098131. <https://doi.org/10.1029/2022GL098131>
- Fueglistaler, S., et al. (2013), The relation between atmospheric humidity and temperature trends for stratospheric water, *J. Geophys. Res. Atmos.*, 118, 1052–1074, doi:10.1002/jgrd.50157.
- Gomez, R. M., G. E. Nedoluha, H. L. Neal, and I. S. McDermid (2012), The fourth-generation Water Vapor Millimeter-Wave Spectrometer, *Radio Sci.*, 47, RS1010, doi:10.1029/2011RS004778.
- Karagodin-Doyennel, A., Rozanov, E., Kuchar, A., Ball, W., Arsenovic, P., Remsberg, E., Jöckel, P., Kunze, M., Plummer, D. A., Stenke, A., Marsh, D., Kinnison, D., and Peter, T.: The response of mesospheric H<sub>2</sub>O and CO to solar irradiance variability in models and observations, *Atmos. Chem. Phys.*, 21, 201–216, <https://doi.org/10.5194/acp-21-201-2021>, 2021.

488 Khaykin, S., et al., (2022), Global perturbation of stratospheric water and aerosol burden by  
 489 Hunga eruption, *Communications Earth & Environment*, (2022) 3:316,  
 490 <https://doi.org/10.1038/s43247-022-00652-x>

491 Lambert, A., et al. (2007), Validation of the Aura Microwave Limb Sounder stratospheric water  
 492 vapor and nitrous oxide data products, *J. Geophys. Res.*, 112, D24S36,  
 493 [doi:10.1029/2007JD008724](https://doi.org/10.1029/2007JD008724).

494 Lee, J. N., Wu, D. L., and Ruzmaikin, A.: Interannual variations of MLS carbon monoxide  
 495 induced by solar cycle, *J. Atmos. Sol.-Terr. Phys.*, 102, 99–104,  
 496 <https://doi.org/10.1016/j.jastp.2013.05.012>, 2013.

497 Livesey, N. J., et al. (2021), Investigation and amelioration of long-term instrumental drifts in  
 498 water vapor and nitrous oxide measurements from the Aura Microwave Limb Sounder (MLS)  
 499 and their implications for studies of variability and trends, *Atmos. Chem. Phys.*, 21, 15409–  
 500 15430, 2021.

501 Millán, L., Santee, M. L., Lambert, A., Livesey, N. J., Werner, F., Schwartz, M. J., et al. (2022).  
 502 The Hunga Tonga-Hunga Ha'apai Hydration of the Stratosphere. *Geophysical Research Letters*,  
 503 49, e2022GL099381. <https://doi.org/10.1029/2022GL099381>.

504 Nedoluha, G. E., Gomez, R. M., Hicks, B. C., Wrotny, J. E., Boone, C., and Lambert, A. (2009):  
 505 Water vapor measurements in the mesosphere from Mauna Loa over solar cycle 23, *J. Geophys.*  
 506 *Res.*, 114, D23303, <https://doi.org/10.1029/2009JD012504>, 2009.

507 Nedoluha, G. E., R. Michael Gomez, D. R. Allen, A. Lambert, C. Boone, and G. Stiller (2013),  
 508 Variations in middle atmospheric water vapor from 2004 to 2013, *J. Geophys. Res. Atmos.*, 118,  
 509 11,285–11,293, [doi:10.1002/jgrd.508](https://doi.org/10.1002/jgrd.508)

510 Nedoluha, Gerald E., R. Michael Gomez, Ian Boyd, Helen Neal, Douglas R. Allen, David  
 511 Siskind, Alyn Lambert, and Nathaniel J. Livesey, (2022). Measurements of Mesospheric Water  
 512 Vapor from 1992 to 2021 at three stations from the Network for the Detection of Atmospheric  
 513 Composition Change, *Journal of Geophysical Research: Atmospheres*, 127, e2022JD037227.  
 514 <https://doi.org/10.1029/2022JD037227>

515 Nedoluha, Gerald E., R. Michael Gomez, Ian Boyd, Helen Neal, Douglas R. Allen, Alyn  
 516 Lambert, and Nathaniel J. Livesey, (2023). Measurements of Stratospheric Water Vapor at  
 517 Mauna Loa and the Effect of the Hunga Tonga Eruption, *Journal of Geophysical Research:*  
 518 *Atmospheres* (in revision).

519 Pumphrey, H. C., et al., Validation of middle-atmosphere carbon monoxide retrievals from the  
 520 Microwave Limb Sounder on Aura, *J. Geophys. Res.*, 112, D24S38, [doi:](https://doi.org/10.1029/2007JD008723)  
 521 [10.1029/2007JD008723](https://doi.org/10.1029/2007JD008723), 2007.

522 Remsberg, E. (2010), Observed seasonal to decadal scale responses in mesospheric water vapor,  
 523 *J. Geophys. Res.*, 115, D06306, [doi:10.1029/2009JD012904](https://doi.org/10.1029/2009JD012904).

- 524 Remsberg, E., Damadeo, R., Natarajan, M., & Bhatt, P. (2018). Observed responses of  
525 mesospheric water vapor to solar cycle and dynamical forcings. *Journal of Geophysical*  
526 *Research: Atmospheres*, 123, 3830–3843. <https://doi.org/10.1002/2017JD028029>
- 527 Schoeberl, M. R., Wang, Y., Ueyama, R., Taha, G., Jensen, E., & Yu, W. (2022). Analysis and  
528 impact of the Hunga Tonga-Hunga Ha'apai stratospheric water vapor plume. *Geophysical*  
529 *Research Letters*, 49, e2022GL100248. <https://doi.org/10.1029/2022GL100248>
- 530 Vömel, Holger, Stephanie Evan, and M. Tully (2022). Water vapor injection into the stratosphere  
531 by Hunga Tonga-Hunga Ha'apai. *Science*. 377. 1444-1447. 10.1126/science.abq2299

Figure 1.



Figure 2.

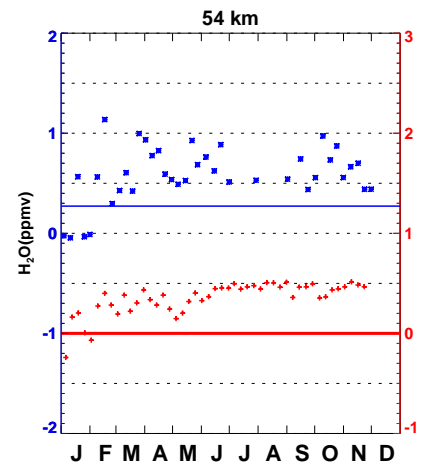
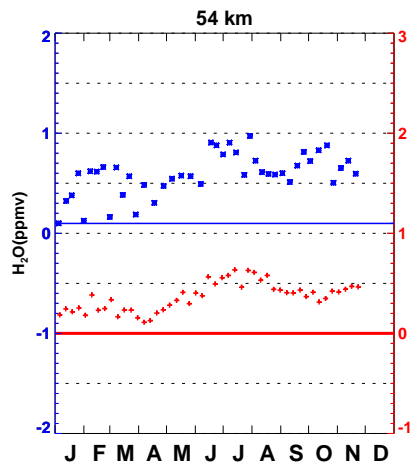
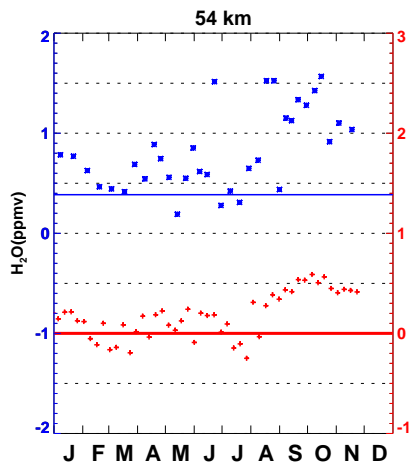
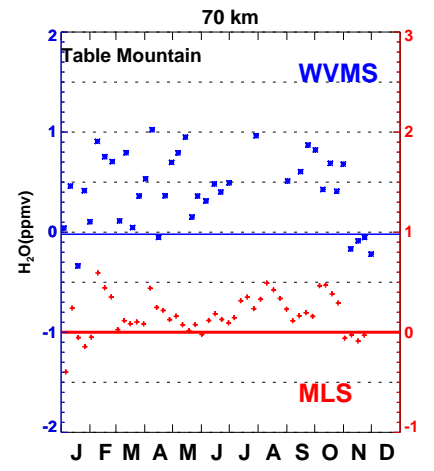
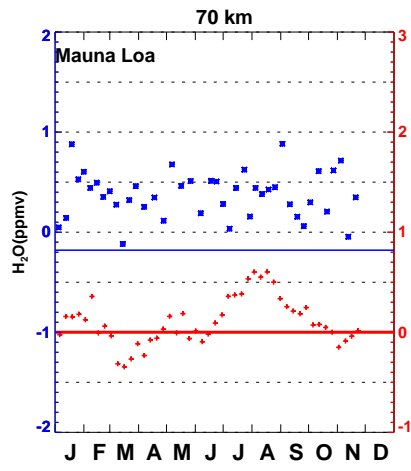
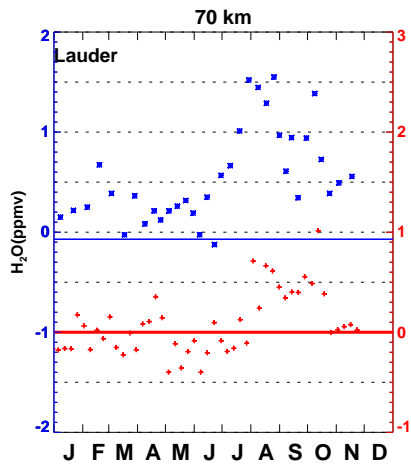


Figure 3.



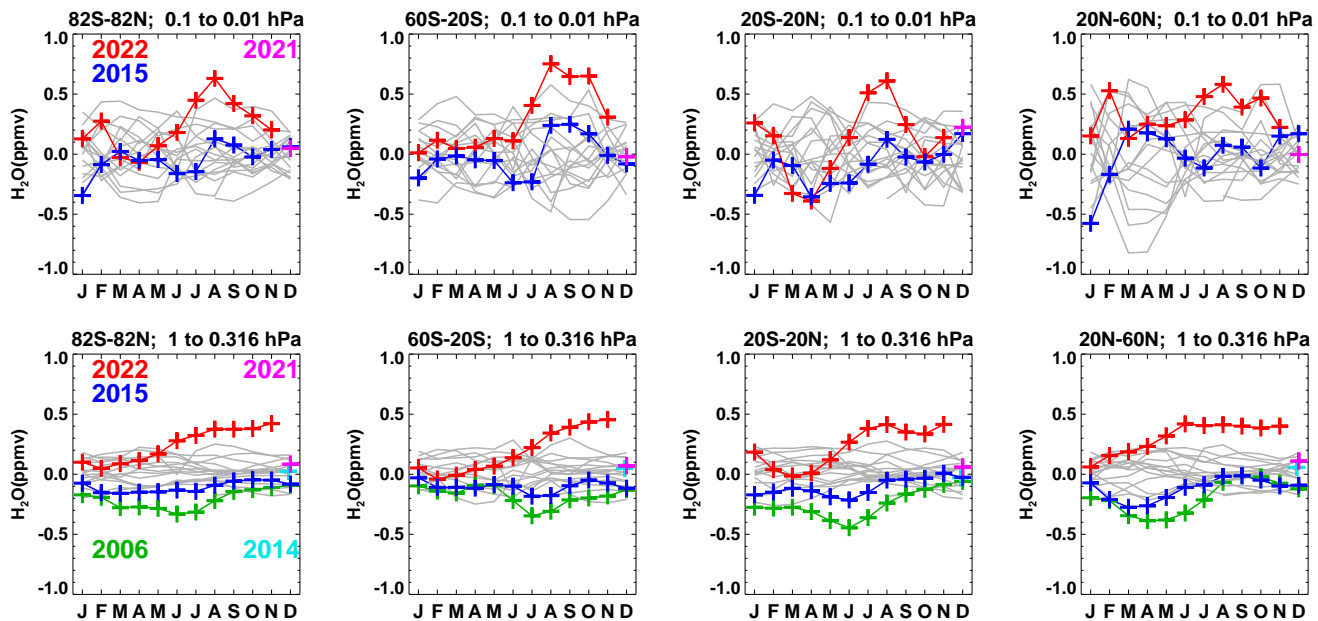


Figure 4.

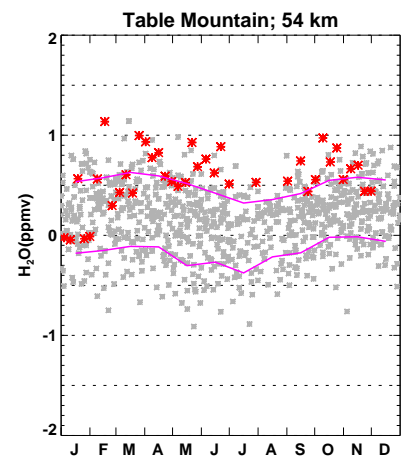
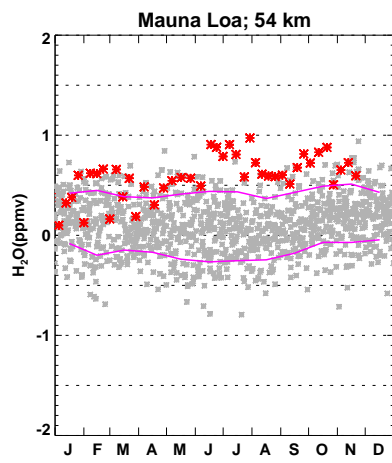
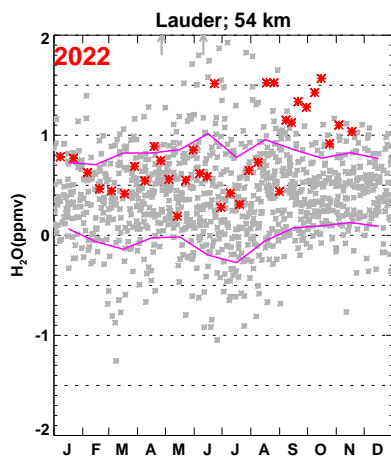
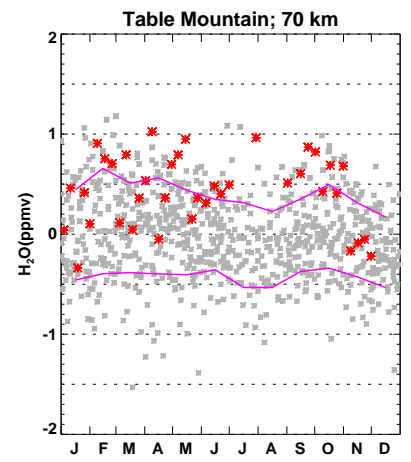
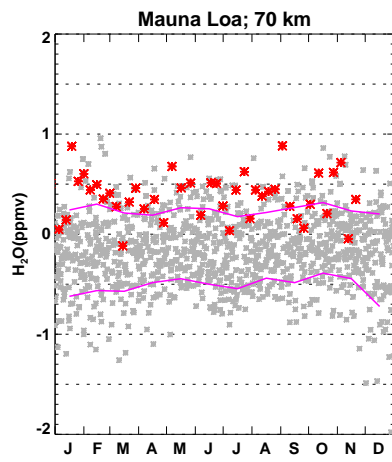
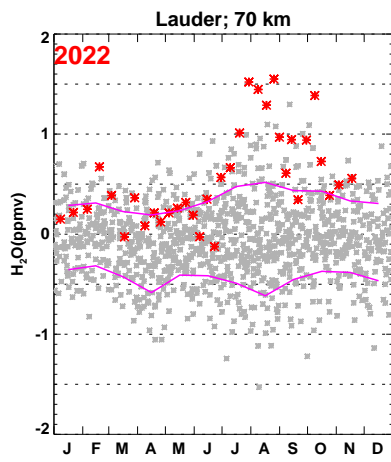


Figure 5.

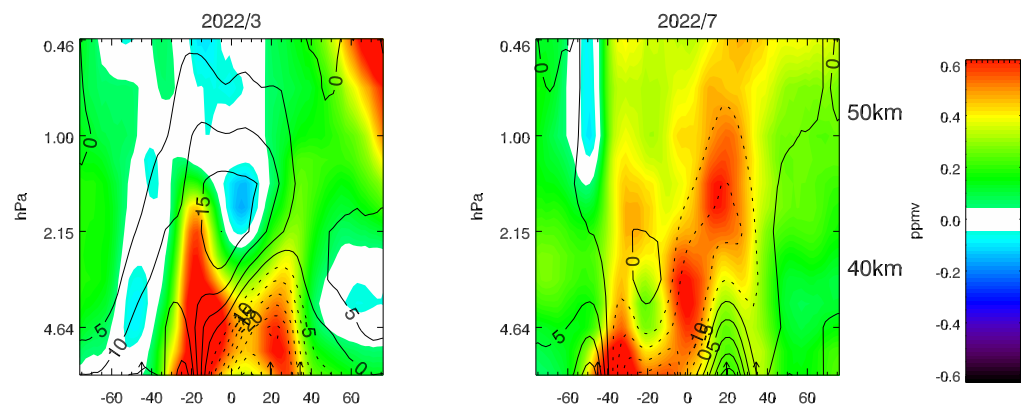


Figure 6.

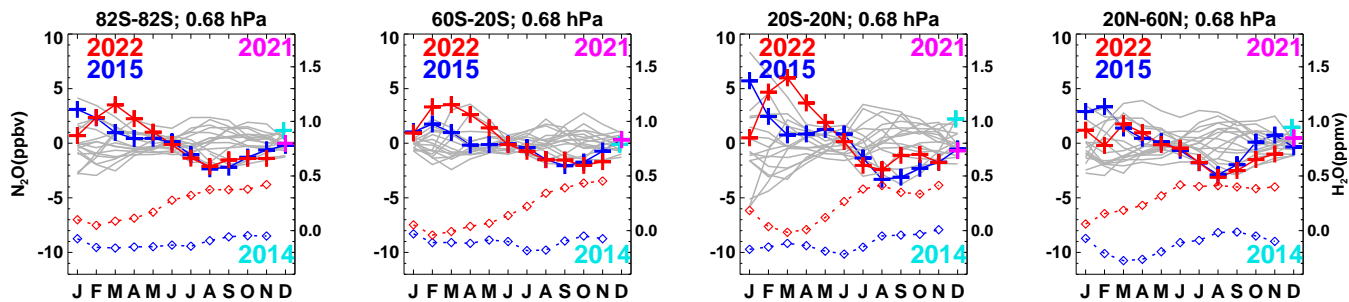


Figure 7.



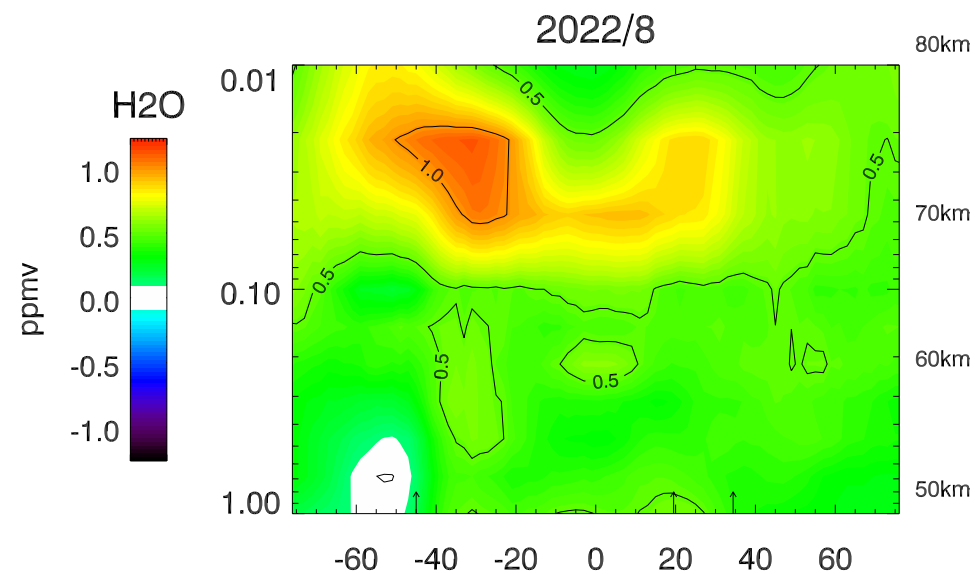
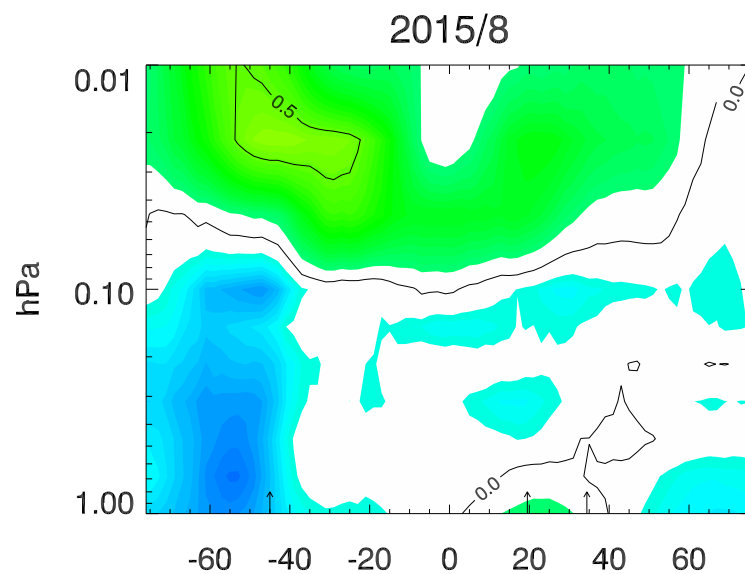
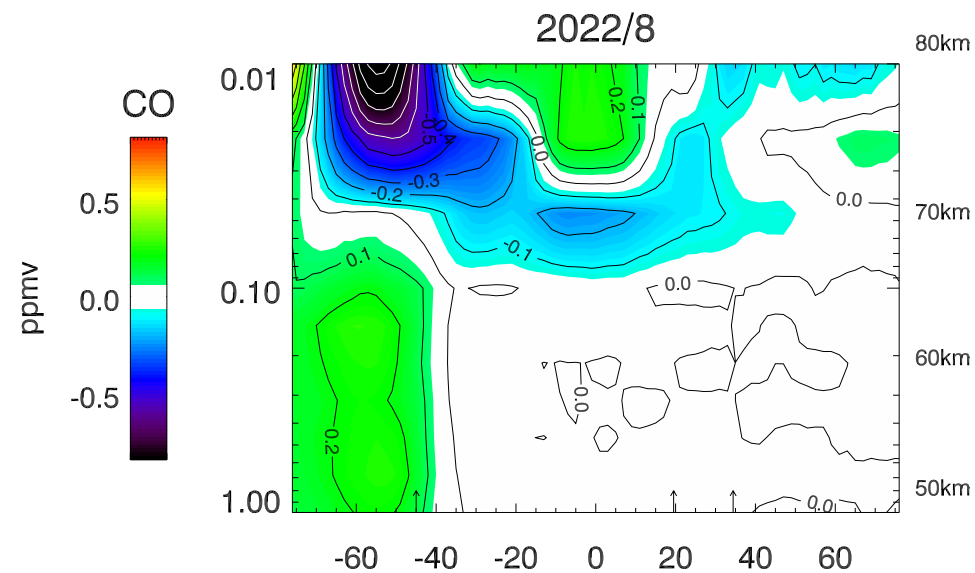
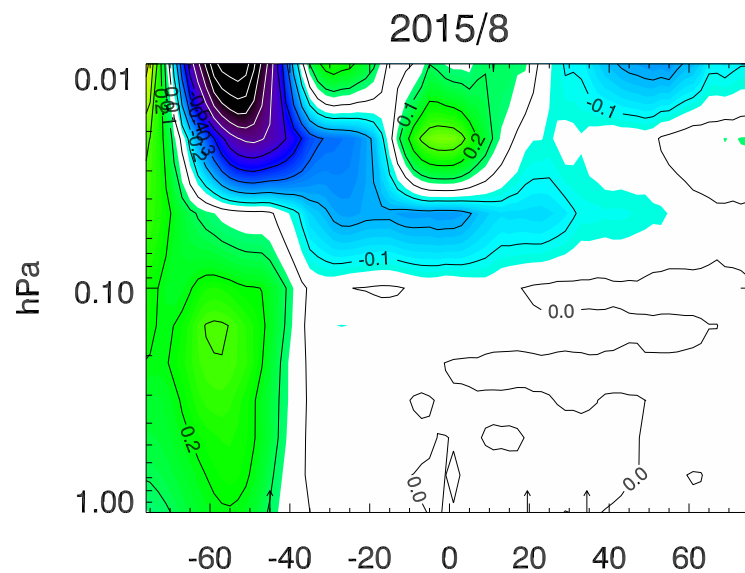


Figure 8.

